Long non-coding RNA MEG3 silencing and microRNA-214 restoration elevate osteoprotegerin expression to ameliorate osteoporosis by limiting TXNIP

Rui Ding
the third affiliated hospital of southern of southern medical univeristy, guangdong provincial key laboratory of bone and joint degeneration diseases, southern medical university, academy of orthopedics of guangdong provinces

ZhengTao Gu
the second affiliated hospital of southern medical univresity,guangdong provincial key laboratory of bone and joint degeneration diseases, southern medical university, academy of orthopaedics of guangdong province

ChangSheng Yang
the second affiliated hospital of southern medical university,guangdong provincial key laboratory of bone and joint degeneration diseases,southern medical university,academy of orthopaedics of guangdong province

CaiQiang Huang
the third affiliated hospital of southern medical university,guangdong provincial key laboratory of bone and jonit degeneration diseases, southern medical university,academy of orthopaedics of guangdong province

QingChu Li
the third affiliated hospital of southern medical university,guangdong provincial key laboratory of bone and jonit degenerationdiseases, southern medical university,academy of orthopaedics of guangdong province

DengHui Xie
the third affiliated hospital of southern medical university,guangdong provincial key laboratory of bone and jonit degeneration diseases,southern medical university,academy of orthopedica of guangdong province

RongKai Zhang
the third affiliated hospital of southern medical university,guangdong provincial key laboratory of bone znd joint degeneration =,southern medical university,academy of orthopaedics of guangdong province

YiYan Qiu (✉ Qiuyiyan2056@163.com)
thee third affiliated hospital of southern medcial university,guangdong provincial key laboratory of bone and joint degeneration diseases,southern medical university, academy of orthopaedics of guangdong

provinces

Research

Keywords: Osteoporosis, Long non-coding RNA maternally expressed gene 3, MicroRNA-214, Thioredoxin-interacting protein, Osteoprotegerin, Osteoblasts, Proliferation, Differentiation

Posted Date: December 18th, 2019

DOI: https://doi.org/10.21203/rs.2.19130/v1

Version of Record: A version of this preprint was published at Journal of Cellular and Molecular Medicine on January 3rd, 2021. See the published version at https://doi.org/10.1111/jcmm.16096.

Abstract

Background

Long non-coding RNAs (LncRNAs) have been found to regulate innumerable diseases, yet the role of lncRNA MEG3 in osteoporosis (OP) has rarely been discussed. Here, we intend to probe into the mechanism of MEG3 on OP development by modulating microRNA-214 (miR-214) and thioredoxin-interacting protein (TXNIP)

Methods

Rat models of OP were established. MEG3, miR-214, and TXNIP mRNA expression in rat femoral tissues was detected, along with TXNIP, PCNA, cyclin D1, OCN, RUNX2, Osteolix, OPG, and PANKL protein expression. Ca, P and ALP contents in rat blood samples were also determined. Primary osteoblasts were isolated and cultured. Viability, COL-I, COL-II and COL-X contents, ALP content and activity, and mineralized nodule area of rat osteoblasts in each group were further detected.

Results

MEG3 and TXNIP were overexpressed while miR-214 was underexpressed in femoral tissues of OP rats. MEG3 silencing and miR-214 overexpression increased BMD, BV/TV, Tb.N, Tb.Th, the number of osteoblasts, collagen area and OPG expression, and downregulated PANKL of femoral tissues in OP rats. MEG3 silencing and miR-214 overexpression elevated Ca and P contents and reduced ALP content in OP rats' blood, elevated viability, differentiation ability, COL-I and COL-X contents and ALP activity, and abated COL-II content of osteoblasts. MEG3 specifically bound to miR-214 to regulate TXNIP.

Conclusion

Collectively, we demonstrated that MEG3 silencing and miR-214 overexpression promote proliferation and differentiation of osteoblasts in OP by downregulating TXNIP, which further improves OP.

Background

Osteoporosis (OP) refers to a systemic disease of bone structures giving rise to low bone mass reduction in bone mass caused by imbalance between bone formation and resorption ratio and the micro architectural deterioration, and it is also a severe health problem leading to great economic and social impacts [1]. There are numerous factors which may account for the occurrence of OP, such as mechanical loading, heritable and nonheritable factors, estrogen deficiency during menopause and aging caused by intracellular reactive oxidative species [2]. In consideration of the stable rise in people's life expectancy and the substantial alterations in people's lifestyles in China in the past years, OP is likely to be more prevalent in the near future [3]. Hence there is a pressing need for us to seek for more effective treatments for OP.

Long non-coding RNAs (LncRNAs) refer to RNA transcripts (> 200 nucleotides) with no or little protein-coding ability which are capable of modulating gene expression via various mechanisms, such as mRNA splicing and epigenetic silencing [4]. A recent report has revealed that lncRNA CRNDE exerts effects on osteoclast proliferation through estrogen deficiency in postmenopausal OP [5]. Also, maternally expressed gene 3 (MEG3), an important lncRNA, has lately been proposed to depress osteogenic differentiation of bone marrow mesenchymal stem cells (BMSCs) in postmenopausal OP via modulating microRNA-133a-3p (miR-133a-3p) [6]. There has been study showing that miR-214 is a target gene of MEG3 [7]. Prior literature has proved that miR-214 contributes to osteoclastogenesis via modulating PTEN/PI3K/AKT pathway [8]. It has also been suggested that miR-214 defends MC3T3-E1 osteoblasts from H_2O_2-induced apoptosis by restricting oxidative stress and regulating ATF4 expression [9]. Thioredoxin-interacting protein (TXNIP), identified as target of miR-244 and miR-452, is a pervasively expressed protein which interacts and negatively modulates Thioredoxin expression and function [10, 11]. Lekva T et al. have proffered that TXNIP knockdown in osteoblasts boosts cell differentiation and osteocalcin (OCN) expression and secretion, and strengthens alkaline phosphatase (ALP) activity [12]. Nicotinamide mononucleotide-mediated repression of TXNIP/NLRP3 inflammasome pathway has been reported to attenuate Aluminum-induced bone loss [13]. Nevertheless, little research has probe into the function of lncRNA MEG3 in OP. Therefore, we performed this study to figure out how MEG3 affects OP development by modulating miR-214 and TXNIP.

Materials And Methods

Ethics statement

Animals were treated humanely using approved procedures in compliance with the recommendations in the Guide for the Care and Use of Laboratory Animals of the National Institutes of Health. The protocol was approved by the Institutional Animal Care and Use Committee of The Third Affiliated Hospital of Southern Medical University, Guangdong Provincial Key Laboratory of Bone and Joint Degeneration Diseases, Southern Medical University, Academy of Orthopedics of Guangdong Province.

Experimental animals

Ninety female rats (3 months old, 226 ± 12 g) purchased from Nanjing Qingzilan Technology Co., Ltd. (Jiangsu, China) were fed on standard feedstuff and kept in cages, free to feed and drink water (12-h day/night cycle, 23-26°C, 40-70% relative humidity). An operation was performed after adaptive feeding in the laboratory.

Modeling of rats

Twenty rats were divided into OP group and sham group. Rats in the OP group were intraperitoneally injected with 1% pentobarbital sodium (0.1 mL/100 g). After completely anesthetized, the rats were fixed in the prone position to cut the clothing hair on the back. After the back skin was disinfected by iodine and alcohol, a longitudinal incision was made on both sides of the spine to separate the muscles and

open the abdominal cavity. Then the left and right ovaries (carnation granules on the adipose tissue) were cut off, and the abdomen was sutured layer by layer with the fur sutured with 2-3 needles on both sides. After erythromycin eye ointment was applied to both eyes, the rats were put back into the cages in the prone position. The rats in the sham group were treated in the same way as above except that the uterus was not ligated and the ovaries were not removed.

Grouping and treatment

Seventy rats were divided into 7 groups (N = 10) [14]: OP group: injection of normal saline 1 w after modeling through tail vein; si-MEG3 group: injection of si-MEG3 1 w after modeling through tail vein; si-negative control (NC) group: injection of si-MEG3 NC 1 w after modeling through tail vein; miR-214 mimics group: injection of miR-214 mimics 1 w after modeling through tail vein; mimics NC group: injection of miR-214 mimics NC 1 w after modeling through tail vein; overexpression (OE)-MEG3 + miR-214 mimics group: injection of OE-MEG3 and miR-214 mimics 1 w after modeling through tail vein; OE-MEG3 + mimics NC group: injection of OE-MEG3 and miR-214 mimics NC 1 w after modeling through tail vein. After 12 w, all rats were euthanatized by cervical dislocation for subsequent indicator detection. All the above plasmids were purchased from GenePharma (Shanghai, China).

Detection of bone histomorphometric indicators

The femurs of all rats were fixed in periodate-L-lysine-paraformaldehyde for 48 h, and then scanned on a CT machine according to relevant parameters. CTAn software was adopted to calculate bone mineral density (BMD), bone surface/bone volume (BS/BV), trabecular bone number (Tb.N), and trabecular thickness (Tb.Th).

Blood sample collection and determination of Ca, P and ALP levels

Before the rats were euthanatized, blood was taken from the vein of posterior eyelid plexus, left for about 1 h, centrifuged at 3000 r/min at 4°C for 15 min to separate serum. The contents of Ca, P and ALP in the blood of each group were detected by an automatic biochemical analyzer.

Bone tissue section preparation

After the muscle connective tissues surrounding 1/3 of the distal femur on the right side of rats were removed, and the bone tissues were placed in 4% paraformaldehyde (pH 7.4, containing 0.1% diethyl pyrocarbonate) for 24 h, and decalcified in 10% ethylenediaminetetraacetic acid (EDTA) at 4°C for 8 w (EDTA was changed once every 4 to 5 d until the tissues became soft). Then, the tissues were immersed in 0.2 mol/L phosphate buffered saline (PBS) overnight, and separately soaked in 70%, 80%, 95% and absolute ethanol mixed with the same volume of n-butyl alcohol for 1 h, then permeabilized in xylene for 30 min, embedded in paraffin, finally sliced into 4-um sections along the longitudinal diameter of the femur and dried.

Hematoxylin-eosin (HE) staining and Masson staining

HE staining: The femurs specimens were dehydrated by alcohol, put in xylene for 10 min, and placed in the dissolved paraffin and then in a dissolved wax tank for heat preservation. Then the specimens were embedded and cut into 5-μm sections, which were then dewaxed with xylene, dehydrated with alcohol of descending concentrations, stained with hematoxylin solution for 5 min, then differentiated in acid water and ammonia water for 10 s, dehydrated in 70% and 90% alcohol for 10 min, and stained with alcohol eosin staining solution for 2-3 min. The stained sections were subsequently dehydrated with absolute ethanol, permeabilized by xylene, sealed by Canadian gum with a cover slip, slightly dried, and finally observed under the microscope.

Masson staining: paraffin sections were dewaxed before chromizing or mercury salt precipitation elimination, which was skipped in tissues fixed with formaldehyde. Then the section were stained with hematoxylin for 5-10 min and with Masson ponceau acid fuchsin solution for 5-10 min, differentiated with 1% phosphomolybdic acid solution for 3-5 min, stained with aniline blue for 5 min, dehydrated with 95% and anhydrous alcohol, and finally observed under the microscope after xylene permeabilization and sealing with neutral gum.

Immunohistochemical staining

The prepared tissue sections were deplasticized, hydrated, and put in 3% H_2O_2 for 10 min to block endogenous peroxidase, and placed into 0.01 M citrate buffer (pH 6.0) for 5-min antigen retrieval under high pressure steam. After cooled for 20 min, the sections were sealed with 5% goat serum for 20 min, supplemented with 40 μL goat anti-osteoprotegerin (OPG) and receptor activator of nuclear factor κB ligand (RANKL) (both 1:150) polyclonal antibody, and placed in a wet box at 4°C overnight, followed by adding biotinylated rabbit anti-goat immunoglobulin G secondary antibody (15 min) and horseradish peroxidase-labeled streptavidin (15 min), and 3-amino-9-ethylcarbazole staining under the microscope. At last, the sections were observed under the microscope after counterstained with hematoxylin and sealed with glycerin gelatin.

Isolation and culture of osteoblasts

On the ultra-clean bench in the cell room, some cancellous bones of the femurs were cut into 2-mm^3 masses by a rongeur and other instruments, placed in a sterile 50 mL centrifuge tube, and then shaken repeatedly and rinsed 3 times with PBS until the cancellous bone granules became white honeycomb. Next, the samples were detached with 0.25% trypsin in an incubator at 37°C for 5 min, washed twice with α-minimum Eagle's medium (α-MEM) containing 10% fetal bovine serum (FBS), and rinsed once with PBS, then detached with 1 mg/mL type II collogen (COL-II) at 37°C for 1.5 h (shaken every 15 min), and then supplemented with α-MEM containing 20% FBS to end the detachment. After centrifugation and 3 washes with α-MEM containing 10% FBS (after each wash, bone tissues and cells were precipitated by centrifugation at 1000 r/min for 10 min), the samples were supplemented the culture solution (α-MEM + 15% FBS + 100 U/mL penicillin + 100 μg/mL streptomycin) and triturated to free more osteoblasts. The cells were separately added 4 to 5 25-cm^2 cell culture flasks after trituration (some cells were separated

and added to cell culture dish with a built-in coverslip, and then type I collagen (COL-I) staining, Gomori staining, alizarin red staining (ARS) were performed for cell identification after the cells spread over the dish).

Osteoblast identification

After reaching confluence, the cells were detached with 0.25% trypsin-EDTA solution and inoculated into a plate with a cover glass at 3×10^5 cells/mL, and the osteoblast phenotype was identified as follows.

COL-I staining: After confluence, the cells were fixed with 4% paraformaldehyde for 10 min, stained with Weigert iron hematoxylin dye solution for 5 min and VanGieson picric acid-acid fuchsin staining solution for 5 min, and rapidly differentiated and dehydrated with 95% ethanol. Then the coverslip was placed under an inverted microscope for observation, and photos were taken.

Gomori staining: After confluence, the cells were fixed with 4% paraformaldehyde for 10 min, incubated at 37°C for 6 h with incubation solution (0.5% β-glycerophosphate, 0.9% calcium chloride, 0.04% magnesium sulfate, 0.5% barbital sodium), treated with 2% nitric acid for 5 min and 1% ammonium sulfide for 1 min, and rapidly differentiated and dehydrated with 95% ethanol. Then the coverslip was placed under an inverted microscope for observation, and photos were taken.

ARS staining: After cell confluence, the supernatant was removed, fixed with 95% ethanol for 2 min, and air-dried. Then 2% alizarin red dye solution was prepared to stain the cells, and the staining reaction was terminated through 3 ddH_2O washes. Then the cells were observed under a microscope, scanned and photographed after dried.

Cell grouping and transfection

The separately cultured osteoblasts in the model group were divided into 7 groups: blank group: no transfection with any sequence; si-MEG3 group: transfection with si-MEG3; si-NC group: transfection of si-MEG3 NC; miR-214 mimics group: transfection with miR-214 mimics; mimics NC group: transfection with miR-214 mimics NC; OE-MEG3 + miR-214 mimics group: transfection with OE-MEG3 and miR-214 mimics; OE-MEG3 + mimics NC group: transfection with OE-MEG3 and miR-214 mimics NC. Normal osteoblasts were also used as a control group.

Transfection: Osteoblasts were transfected after added to a sterile 6-well culture plate at 5×10^5-1×10^6 cells for 20-h culture to reach 70% confluence rate. Before transfection, the cells were washed twice with PBS to completely remove the serum-containing medium, and 1 mL of serum-free medium was added to each well for 4-h culture (37°C, 5% CO_2). Then 6 sterile Eppendorf (EP) tubes were used to prepare serum-free dilutions of Lipofectamine 2000 (Thermo Fisher Scientific, Waltham, MA, USA), and the another 6 to prepare serum-free dilutions of si-MEG3, si-NC, miR-214 mimics, mimics NC, OE-MEG3 + miR-214 mimics and OE-MEG3 + mimics NC. Then the liquids in the latter 6 tubes were separately mixed with Lipofectamine 2000 in the former tubes within 5 min, gently mixed, and incubated for 20 min to form an

RNA-Lipofectamine complex. After the incubation, 500 μL of RNA-Lipofectamine complex was added to each well and mixed evenly. After 6-h incubation at 37°C with 5% CO_2, the medium was replaced with fresh medium containing 10% FBS to continue the culture. After 48 h, cells were collected for subsequent experiments.

3-(4,5-dimethylthiazol-2-yl)-2,5-diphenyltetrazolium bromide (MTT) assay

Osteoblasts (1 mL) in each group in logarithmic phase was inoculated in a 96-well cell culture plate at 1 × 10^5 cells/mL, and incubated for 24 h. After cell attachment, the medium was substituted with 200 μL Dulbecco's modified Eagle's medium/F12 with 10% FBS and incubated with MTT solution (20 μL, 5 mg/mL) for 4 h at 37°C. After removing the supernatant, 150 μL dimethyl sulphoxide was added to each well, shaken at low speed for 10 min, and an microplate reader was adopted to detect the optical density (OD) value at 490 nm. Three independent replicate experiments were performed.

5-ethynyl-2'-deoxyuridine (EdU) staining

Osteoblasts were collected, counted, inoculated in 6-well plates at 2 × 10^2 cells/mL, and incubated in a shaker for 0.5 h with 100 μL 1 ´ Apollo staining reaction solution prepared according to the kit instructions (Invitrogen, CA, USA) without light and then with PBS for 10 min. Next, each well was supplemented with 5 μL 1 ´ Hoechst 33342 reaction solution for 0.5-h incubation avoiding light and then with 100 μL penetrant (0.5% Triton X) for 2 to 3 times of incubation in a shaker (10 min/time). After 10-min incubation with 100 μL PBS, the cells were incubated with Apollo staining solution in the dark and observed by a fluorescence microscopy to calculate proliferative cells. Three slides were observed in each group, and 200 cells were randomly observed on each slide. The proliferation rate (%) = number of proliferative cells (red)/number of observed cells (blue) ´ 100%. The number of cells was counted by Image-Pro Plus 6.0. When the cells were in the phase of DNA synthesis, they were stained red and the nuclei were blue. The cells in the S phase were light red after the overlap of the pictures.

Immunocytochemical detection of COL-I, COL-II and COL-X contents

Referring to the specifications of diaminobenzidine (DAB)-0031 immunocytochemistry kit (MXB, Fujian, China), the prepared cell slides were placed in PBS for 10 min, and immersed in 3% H_2O_2 for 15 min to block endogenous catalase. Primary antibodies (COL-I, COL-II, COL-X) were diluted according to the specifications (Abcam, Cambridge, UK), which were then added to each slide (50 μL) and incubated in a wet box at 4°C overnight. The next day, the slides were rewarmed at room temperature for 0.5 h. After removing the free primary antibody and excess liquid, the second antibodies (5 μL) were added one by one according to the specifications and kept at room temperature for 0.5 h. After removing the free secondary antibody, the mixture was stained with the prepared DAB-peroxidase color developer for 5 min and with hematoxylin for 3 min, differentiated with 1 % hydrochloric acid alcohol for 15-30 s, dehydrated by concentration gradient ethanol and permeabilized with xylene, followed by sealing with neutral gum and observation under the microscope. The cell membrane, nucleus or cytoplasm attached by brown particles were positive, otherwise they're negative.

ALP staining with 5-bromo-4-chloro-3-indolyl phosphate (BCIP)/nitrotetrazolium blue chloride (NBT) kits

Osteoblasts in logarithmic phase were inoculated into a 6-well plate at 1.0×10^5 cells/well, and the medium was altered every 2 to 3 d. When the cell confluence was 60%, osteoblasts were fixed with 95% ethanol for 2 min and then dried. Then 2 mL BCIP/NBT staining working solution prepared at the reference ratio in the specifications (Nanjing Jiancheng Bioengineering Institute, Nanjing, China) was added add to be fully spread over the surface, and incubated at room temperature or 37°C in the dark for 5-30 min until the color development was normal. After removing the BCIP/NBT staining working solution, the staining was ended by 1-2 ddH_2O washes, and the experimental results were recorded.

Reverse transcription quantitative polymerase chain reaction (RT-qPCR)

Trizol (Invitrogen, Carlsbad, CA, MSA) one-step method was adopted to extract total RNA from tissues and cells, and NanoDrop2000 (Thermo Fisher Scientific, Waltham, MA, USA) to determine the concentration and quality of RNA. RNA was reversely transcribed into cDNA according to the reverse transcription kit ReverTra Ace qPCR RT Kit (TOYOBO, Osaka, Japan) and stored at 4°C. RT-PCR reaction system was prepared based on the Sybr green kit (Takara, Dalian, China), and the primers were synthesized by BGI (Guangdong, China) (Table 1). MEG3 and miR-214 were expressed relative to U6, and TXNIP relative to glyceraldehyde-3-phosphate dehydrogenase (GAPDH). The PCR amplification products were verified by agarose gel electrophoresis. threshold cycle (Ct) value of each test tube was obtained by manually setting the threshold at the lowest point of each parallel rising logarithmic amplification curve, and the data were analyzed by $2^{-\Delta\Delta Ct}$ method. The experiment was repeated three times, and the data were averaged.

Western blot analysis

Total protein of tissues and cells in each group were extracted, and protein concentration was measured with the bicinchoninic acid protein concentration determination kit (Beyotime Institute of Biotechnology, Shanghai, China). Then OD value of each well was measured at 570 nm with a microplate reader, and the concentration of each sample was calculated. After the protein concentration in each group was adjusted to the same level, the extracted protein was added to the loading buffer and boiled at 95°C for 10 min, and each well was then loaded with 30 μg sample. Next, the protein was separated by 10% polyacrylamide gel electrophoresis (80 V for 30 min, then 120V), transformed to polyvinylidene fluoride (PVDF) membrane (300 mA, 60-120 min) in ice water, and blocked in 5% bovine serum albumin for 2 h. Primary antibody TXNIP, proliferating cell nuclear antigen (PCNA), cyclin D1, OCN, runt-related transcription factor 2 (RUNX2), Osteolix,, OPG (all 1:1000) and GAPDH (1:3000) (all from Abcam, Cambridge, MA, USA) were added and kept at 4°C overnight, and then the corresponding diluted secondary antibody (MT-BIO, Shanghai, China) was added and incubated for 2 h, followed by development with chemiluminescent reagent. GAPDH was used as the internal reference. Gel Doc EZ Imager (Bio-rad, California, USA) was applied for development, and the gray values of target bands were analyzed by Image J software. The experiment was repeated three times and the data were averaged.

Dual luciferase reporter gene assay

The binding site of lncRNA MEG3 and miR-214 were predicted and analyzed at the bioinformatics website, which was then verified by dual luciferase reporter gene assay. The synthetic MEG3 3'untranslated regions (3'UTR) gene fragment was introduced into the pMIR-reporter (Beijing Huayueyang Biotechnology Co., Ltd., Beijing, China) via endonuclease sites (Bamh1 and Ecor1). The complementary sequence mutation site of the seed sequence was designed on the wild type (WT) of MEG3, and the target fragment was inserted into the pMIR-reporter plasmid by T4 DNA ligase after restriction endonuclease digestion. Then the WT and mutant type (MUT) luciferase reporter plasmids with correct sequence were independently co-transfected with mimics NC and miR-214 mimics into osteoblasts. After 48 h, cells were lysed, and luciferase activity was measured with luciferase assay kit (BioVision, San Francisco, CA, USA) and Glomax20/20 luminometer (Promega, Madison, Wisconsin, USA). The experiment was repeated three times.

The targeting relationship of miR-214 and TXNIP and the binding site of miR-214 and TXNIP 3'UTR were predicted with a bioinformatics software (https://cm.jefferson.edu/rna22/Precomputed). The TXNIP 3'UTR promoter sequence containing the miR-214 binding site was synthesized, and a TXNIP 3'UTR WT plasmid (TXNIP WT) was constructed. Based on this plasmid, TXNIP 3'UTR MUT plasmid (TXNIP MUT) was established by mutating the binding site. TXNIP WT and TXNIP MUT were extracted in light of the specifications of plasmid extraction kit (Promega, Madison, Wisconsin, USA). Osteoblasts in logarithmic phase were inoculated in 96-well plates, and transfected with the mixtures of TXNIP WT and TXNIP MUT with mimics NC and miR-214 mimics respectively, by Lipofectamine 2000 (Invitrogen, Carlsbad, CA, USA) at about 70% cell density. Forty-eight hours later, cells were lysed, and luciferase activity was detected with a luciferase assay kit (BioVision, San Francisco, CA, USA).

RNA pull-down assay

Three different biotin-labeled miRNA sequences (WT miR-214 [Bio-miR-214-WT], MUT miR-214 [Bio-miR-214-MUT], sequence mutation complementary to lncRNA MEG3], and a random miRNA not complementary to MEG3 [Bio-NC] as a NC) were designed and synthetized. The osteoblasts were transfected with the above three miRNAs at 80%-90% cell density. After 48 h, protein cleavage products were obtained from cell lysate by lysing cells with lysis buffer. Then the lysate was incubated with streptavidin-coated magnetic beads (M-280, Sigma-Aldrich, St. Louis, MO, USA) for 3 h at 4°C. Finally, the protein-nucleic acid compound adsorbed by magnetic beads was eluted, and the total RNA was extracted with Trizol, with MEG3 expression detected by RT-qPCR. Each experiment was repeated three times.

Statistical analysis

Data were analyzed with SPSS 21.0 (IBM Corp., Armonk, NY, USA). The measurement data were expressed as mean ± standard deviation. The data subjected to normal distribution between two groups were compared by t-test, and those among multiple groups were analyzed by one-way analysis of

variance (ANOVA), after which pairwise comparison was performed by the least significant difference t-test (LSD-t) method. *P* was a two-sided test, and the difference was statistically significant at $P < 0.05$.

Results

MEG3 and TXNIP are overexpressed while TXNIP is underexpressed in femoral tissues of OP rats

MEG3, miR-214 and TXNIP expression of rat femoral tissues in each group was detected by RT-qPCR and Western blot analysis (Figure 1A-E). The results showed that MEG3 and TXNIP expression was pronouncedly enhanced while miR-214 expression was largely lowered in the OP group relative to the sham group, and MEG3 and TXNIP expression was clearly reduced while miR-214 expression was obviously augmented in the si-MEG3 group in relation to the NC group (all $P < 0.05$). In contrast to the NC groups, MEG3 expression suggested almost no changes (both $P > 0.05$), and TXNIP was evidently downregulated while miR-214 was markedly upregulated in the miR-214 mimics and OE-MEG3 + miR-214 mimics groups (all $P < 0.05$).

MEG3 silencing and miR-214 overexpression enhance BMD, BV/TV, Tb.N and Tb.Th of femoral tissues in OP rats

The indicators of rat femoral tissues in each group were analyzed by micro-CT (Figure 2A-E). The results indicated that BMD, BV/TV, Tb.N and Tb.Th in rat femoral tissues suggested a great drop in the OP versus the sham group, yet a palpable rise in the si-MEG3, miR-214 mimics and OE-MEG3 + miR-214 mimics groups versus the NC groups (all $P < 0.05$)

MEG3 silencing and miR-214 overexpression elevate Ca and P contents and reduce ALP content in OP rats' blood

The contents of Ca, P and ALP in rat's blood of each group were detected by the automatic biochemical analyzer (Figure 3A-C). The findings revealed that Ca and P contents suggested a decline while ALP content showed a rise in the OP group versus the sham group, yet Ca and P contents showed elevation while ALP content suggested abatement in the si-MEG3, miR-214 mimics and OE-MEG3 + miR-214 mimics groups versus the NC groups (all $P < 0.05$)

MEG3 silencing and miR-214 overexpression increase the number of osteoblasts and collagen area of femoral tissues in OP rats

The structure of rat femoral tissues in each group was observed through HE staining and Masson staining (Figure 4AB). The number of osteoblasts and collagen area in rat femur suggested distinct abatement in the OP group versus the sham group, yet notable elevation in the si-MEG3, miR-214 mimics and OE-MEG3 + miR-214 mimics groups versus the NC groups (all $P < 0.05$)

MEG3 silencing and miR-214 overexpression upregulate OPG protein expression and downregulate PANKL protein expression of femoral tissues in OP rats

Immunohistochemical staining and Western blot analysis were performed to detect OPG and PANKL protein expression in rat femoral tissues (Figure 5A-C). The results revealed that OPG protein expression showed a fall while PANKL protein expression suggested an increase in the OP group versus the sham group, yet OPG protein expression was elevated while PANKL protein expression was lessened in the si-MEG3, miR-214 mimics and OE-MEG3 + miR-214 mimics groups versus the NC groups (all $P < 0.05$)

Results of osteoblast isolation

Under the inverted microscope, on the 7^{th} d after the isolation and culture, the cells climbed out of the femoral tissues and were in the shape of short spindle (Figure 6A). The primary cells crawling out merged into a single layer after detachment and were then passaged. The cells attached to the culture dish within 2 to 4 h and most showed polygonal, shortly fusiform and cuboid shapes. When spreading over the bottom of the bottle, the cells were in fusiform or cuboid shapes and were closely arranged. As the culture time was prolonged, the cells grew in an overlapping and colony-like manner (Figure 6B). The cells were then identified by COL-I staining, Gomori staining, and ARS staining. The results showed cells were stained brownish red in the VanGieson picric acid-acid fuchsin staining, indicating that cells had the function of synthesizing matrix proteins (Figure 6C); there were black particles in the cytoplasm, and a few dispersed around the cells, indicating that the ALP activity of cells improved and the cell bone matrix was matured (Figure 6D). When the cells were confluent, they were stacked in multiple layers, and showed the shape of short column or square; the cells were aggregated locally to form focus and calcified nodules, and showed orange-red particles or massive precipitates after staining (Figure 6E).

MEG3 silencing and miR-214 overexpression strengthen osteoblast viability

PCNA and cyclin D1 protein expression of osteoblasts was detected by Western blot analysis (Figure 7A,B), and osteoblast viability was detected by MTT assay and EdU staining (Figure 7C-E). The results showed that PCNA and cyclin D1 protein expression and osteoblast viability weakened in the blank group versus the control group, and strengthened in the si-MEG3, miR-214 mimics and OE-MEG3 + miR-214 mimics groups versus the NC groups (all $P < 0.05$).

MEG3 silencing and miR-214 overexpression enhance COL-I and COL-X contents and decrease COLII content of osteoblasts

Immunocytochemistry was adopted to detect COL-I, COL-II and COL-X contents of osteoblasts in each group (Figure 8A,B). The results revealed that COL-I and COL-X contents showed diminution while COL-II content suggested enhancement in the blank group versus the control group, yet COL-I and COL-X contents increased while COL-II content reduced in the si-MEG3, miR-214 mimics and OE-MEG3 + miR-214 mimics groups versus the NC groups (all $P < 0.05$).

MEG3 silencing and miR-214 overexpression improve osteoblast differentiation ability

OCN, RUNX2 and Osteolix protein expression of rat osteoblasts in each group were detected by Western blot analysis (Figure 9A,B); ALP staining with BCIP/NBT kits was used to qualitatively and quantitatively analyze osteoblast ALP content and activity, and ARS staining to detect mineralized nodule area of osteoblasts (Figure 9C-E). The results suggested that OCN, RUNX2 and Osteolix protein expression, ALP content and activity and mineralized nodule area of rat osteoblasts diminished in the blank group versus the control group, indicating decreased osteoblast differentiation ability, and the same parameters grew in the si-MEG3, miR-214 mimics and OE-MEG3 + miR-214 mimics groups versus the NC groups, suggesting improved osteoblast differentiation ability (all $P < 0.05$).

MEG3 specifically binds to miR-214

Bioinformatics software was adopted to predict the specific binding region of MEG3 sequence to the miR-214 sequence (Figure 10A). The results from further confirmation by dual luciferase reporter gene assay revealed that the luciferase activity of the MEG3-WT + miR-214 mimics group lowered vs the mimics NC group ($P < 0.05$), and that of the mutant MEG3-MUT + miR-214 mimics group showed few alterations ($P > 0.05$), indicating a binding relationship between MEG3 and miR-214 (Figure 10B).

The results from further verification by RNA-pull down assay revealed that in relation to the Bio-NC group, MEG3 expression in the Bio-miR-214-WT group ascended ($P < 0.05$), yet showed few changes in the Bio-miR-214-MUT group ($P > 0.05$) (Figure 10C).

We also conducted RT-qPCR to determine MEG3 and miR-214 expression in each group (Figure 10D). The results indicated that MEG3 expression ascended while miR-214 expression descended in the OP group versus the sham group, and MEG3 expression went down while miR-214 expression went up in the si-MEG3 group in relation to the NC group (all $P < 0.05$). In relation to the NC groups, MEG3 expression suggested nearly no changes (both $P > 0.05$), and miR-214 expression rose in the miR-214 mimics and OE-MEG3 + miR-214 mimics groups (all $P < 0.05$).

MiR-214 targets TXNIP

The binding site between TXNIP and miR-214 was predicted at https://cm.jefferson.edu/rna22/Precomputed (Figure 11A), and dual luciferase reporter gene assay was adopted to verify that TXNIP was the target gene of miR-214. The results showed that the luciferase activity of osteoblasts co-transfected with miR-214 mimics and TXNIP WT declined ($P < 0.05$) versus the NC group (Figure 11B), indicating miR-214 specifically binds to the TXNIP.

TXNIP expression of transfected osteoblasts in each group was detected by RT-qPCR and Western blot analysis (Figure 11C-E). The results showed that TXNIP expression increased in the OP group versus the sham group, yet fell in the si-MEG3, miR-214 mimics and OE-MEG3 + miR-214 mimics groups versus the NC groups (all $P < 0.05$).

Discussion

OP, a ubiquitous public health problem (especially in women), is characterized by reduced bone strength which is easy to lead to an incremental risk for fracture [15]. Recently, lncRNAs have been confirmed as a novel regulatory code for OP [16]. Here, we discussed the mechanism of lncRNA MEG3 on OP via miR-214 and TXNIP. Collectively, we demonstrate that knockdown of MEG3 and elevation of miR-214 enhance OPG expression, and boost proliferation and differentiation of osteoblasts in OP by downregulating TXNIP, which further improves OP.

To start with, we conducted assays to found that lncRNA MEG3 and TXNIP were overexpressed while miR-214 was underexpressed in femoral tissues of OP rats. Similar to our results, a recent study has showed that MEG3 is upregulated in postmenopausal OP [6]. Another study by Cai N *et al.* has proposed that lncRNA ANCR expression is also augmented in postmenopausal OP [17]. There has been evidence proving that miR-214 expression is low in some disease, such as ovarian cancer and breast cancer [18, 19]. In a previous study, Lekva T *et al.* has reported the high TXNIP mRNA level in Cushing's syndrome [20]. TXNIP has also been documented to be overexpressed in hepatocyte ischemia reperfusion injury [21]. What's more, we also discovered that MEG3 specifically bound to miR-214 to modulate TXNIP expression, and reduced MEG3 expression caused a rise in miR-214 expression which could declined TXNIP expression. Studies have shown that MEG3 works as a ceRNA of miR-214 and decreased MEG3 expression augments miR-214 expression [22]. It has also been indicated that TXNIP is miR-224' target and miR-224 negatively modulates TXNIP expression [23].

To better figure out the mechanism of lncRNA MEG3 on OP development, si-MEG3 and miR-214 mimics were introduced into assays performed in femoral tissues in OP rats and osteoblasts. We found that MEG3 silencing and miR-214 overexpression increased BMD, BV/TV, Tb.N, Tb.Th, the number of osteoblasts, collagen area and OPG expression, and downregulated PANKL of femoral tissues in OP rats. What was also discovered in our study was that MEG3 silencing and miR-214 overexpression elevated Ca and P contents and reduced ALP content in OP rats' blood, elevated viability, differentiation ability, COL-I and COL-X contents and ALP activity, and abated COL-II content of osteoblasts. In addition, we combined OE-MEG3 and miR-214 mimics in our assays, and found that miR-214 restoration counteracts the effects of MEG3 upregulation on OP and osteoblasts. In line with our results, a recent report has revealed that MEG3 silencing increases the levels of COL10A1, Runx2, Osterix and OCN, which speeds up tibia fraction healing [24]. Evidence has shown that lncRNA ANCR silencing enhances the proliferation, calcium deposition and ALP activity and diminished apoptosis of osteoblasts, which facilitates the osteogenesis of osteoblast in postmenopausal OP by modulating EZH2 and RUNX2 [17]. Some researchers have also proffered that diminution of MEG3 catalyzes endothelial differentiation of BMSCs in restoring erectile dysfunction [25]. In addition, Wang Y *et al.* have demonstrated that MEG3 knockdown limits osteosarcoma cell development via modulating miR-127 [26]. A prior study has suggested that lncRNA MEG3 upregulation dampens the osteogenic differentiation of periodontal ligament cells [27]. It has been shown that restoration of miR-214 contributes to osteoclast differentiation [28]. Beside, there has been literature recording that in cervical cancer, miR-214 controls cancer cell growth and invasion by downregulating ARL2 [29]. Furthermore, miR-214 increases breast cancer cell apoptosis and sensitivity to doxorubicin via modulating the RFWD2-p53 cascade [30].

Conclusion

All in all, we reveal that knockdown of MEG3 and elevation of miR-214 strengthen OPG expression, and boost proliferation and differentiation of osteoblasts in OP by downregulating TXNIP, thus mitigating OP. Our study promotes better understanding of the function of MEG3/miR-214/TXNIP axis in OP development and provides new clues for OP treatment. However, in-depth research has to be made to further elaborate the mechanism of lncRNA MEG3 on OP development.

Abbreviations

LncRNAs: Long non-coding RNAs

OP: osteoporosis

TXNIP: thioredoxin-interacting protein

MEG3: maternally expressed gene 3

BMSCs: bone marrow mesenchymal stem cells

miR-133a-3p: microRNA-133a-3p

OCN: osteocalcin

NC: negative control

BMD: bone mineral density

BS/BV: bone surface/bone volume

Tb.N: trabecular bone number

Tb.Th: trabecular thickness

EDTA: ethylenediaminetetraacetic acid

PBS: phosphate buffered saline

HE: Hematoxylin-eosin

α-MEM:α-minimum Eagle's medium

FBS: fetal bovine serum

EP: Eppendorf

OD: optical density

DAB: diaminobenzidine

NBT: nitrotetrazolium blue chloride

RT-qPCR: Reverse transcription quantitative polymerase chain reaction

PVDF: polyvinylidene fluoride

3’UTR: 3’untranslated regions

WT: wild type

MUT: mutant type

ANOVA: analysis of variance

LSD-t: least significant difference t-test

Declarations

Funding

The current research was funded by Project supported by the National Science Foundation for young Scientists of China(Grant No.8180090642)

Competing interests

The authors declare that they have no competing interests.

Ethical Approval and Consent to participate

This study was approved and supervised by the animal ethics committee of The Third Affiliated Hospital of Southern Medical University, Guangdong Provincial Key Laboratory of Bone and Joint Degeneration Diseases, Southern Medical University, Academy of Orthopedics of Guangdong Province. The treatment of animals in all experiments conforms to the ethical standards of experimental animals.

Consent for publication

Not applicable

Availability of supporting data

Not applicable

Authors' contributions

guarantor of integrity of the entire study：Rui Ding

study design：ZhengTao Gu, ChangSheng Yang, CaiQiang Huang

experimental studies：QingChu Li, DengHui Xie, RongKai Zhang

manuscript editing：YiYan Qiu

All authors read and approved the final manuscript.

Acknowledgement

We would like to acknowledge the reviewers for their helpful comments on this paper.

References

1. Straka, M., et al., *Periodontitis and osteoporosis.* Neuro Endocrinol Lett, 2015. **36**(5): p. 401-6.
2. Armas, L.A. and R.R. Recker, *Pathophysiology of osteoporosis: new mechanistic insights.* Endocrinol Metab Clin North Am, 2012. **41**(3): p. 475-86.
3. Wang, Y., et al., *Osteoporosis in china.* Osteoporos Int, 2009. **20**(10): p. 1651-62.
4. Li, W., P. Xie, and W.H. Ruan, *Overexpression of lncRNA UCA1 promotes osteosarcoma progression and correlates with poor prognosis.* J Bone Oncol, 2016. **5**(2): p. 80-5.
5. Li, W., et al., *CRNDE impacts the proliferation of osteoclast by estrogen deficiency in postmenopausal osteoporosis.* Eur Rev Med Pharmacol Sci, 2018. **22**(18): p. 5815-5821.
6. Wang, Q., et al., *LncRNA MEG3 inhibited osteogenic differentiation of bone marrow mesenchymal stem cells from postmenopausal osteoporosis by targeting miR-133a-3p.* Biomed Pharmacother, 2017. **89**: p. 1178-1186.
7. Fan, F.Y., et al., *The inhibitory effect of MEG3/miR-214/AIFM2 axis on the growth of T-cell lymphoblastic lymphoma.* Int J Oncol, 2017. **51**(1): p. 316-326.
8. Zhao, C., et al., *miR-214 promotes osteoclastogenesis by targeting Pten/PI3k/Akt pathway.* RNA Biol, 2015. **12**(3): p. 343-53.
9. Lu, X.Z., et al., *MiR-214 protects MC3T3-E1 osteoblasts against H2O2-induced apoptosis by suppressing oxidative stress and targeting ATF4.* Eur Rev Med Pharmacol Sci, 2017. **21**(21): p. 4762-4770.
10. Knoll, S., et al., *E2F1 induces miR-224/452 expression to drive EMT through TXNIP downregulation.* EMBO Rep, 2014. **15**(12): p. 1315-29.
11. Alhawiti, N.M., et al., *TXNIP in Metabolic Regulation: Physiological Role and Therapeutic Outlook.* Curr Drug Targets, 2017. **18**(9): p. 1095-1103.
12. Lekva, T., et al., *TXNIP is highly regulated in bone biopsies from patients with endogenous Cushing's syndrome and related to bone turnover.* Eur J Endocrinol, 2012. **166**(6): p. 1039-48.

13. Liang, H., et al., *Nicotinamide mononucleotide alleviates Aluminum induced bone loss by inhibiting the TXNIP-NLRP3 inflammasome.* Toxicol Appl Pharmacol, 2019. **362**: p. 20-27.
14. Liu, H.C., et al., *Role of recombinant plasmid pEGFP-N1-IGF-1 transfection in alleviating osteoporosis in ovariectomized rats.* J Mol Histol, 2013. **44**(5): p. 535-44.
15. Jackson, R.D. and W.J. Mysiw, *Insights into the epidemiology of postmenopausal osteoporosis: the Women's Health Initiative.* Semin Reprod Med, 2014. **32**(6): p. 454-62.
16. Wu, Q.Y., et al., *Long Non-coding RNAs: A New Regulatory Code for Osteoporosis.* Front Endocrinol (Lausanne), 2018. **9**: p. 587.
17. Cai, N., C. Li, and F. Wang, *Silencing of LncRNA-ANCR Promotes the Osteogenesis of Osteoblast Cells in Postmenopausal Osteoporosis via Targeting EZH2 and RUNX2.* Yonsei Med J, 2019. **60**(8): p. 751-759.
18. Liu, Y., et al., *MiR-214 suppressed ovarian cancer and negatively regulated semaphorin 4D.* Tumour Biol, 2016. **37**(6): p. 8239-48.
19. Yi, S.J., L.L. Li, and W.B. Tu, *MiR-214 negatively regulates proliferation and WNT/beta-catenin signaling in breast cancer.* Eur Rev Med Pharmacol Sci, 2016. **20**(24): p. 5148-5154.
20. Lekva, T., et al., *Thioredoxin interacting protein is a potential regulator of glucose and energy homeostasis in endogenous Cushing's syndrome.* PLoS One, 2013. **8**(5): p. e64247.
21. Zhang, Y., et al., *TXNIP knockdown alleviates hepatocyte ischemia reperfusion injury through preventing p38/JNK pathway activation.* Biochem Biophys Res Commun, 2018. **502**(3): p. 409-414.
22. Zhu, X., et al., *lncRNA MEG3 promotes hepatic insulin resistance by serving as a competing endogenous RNA of miR-214 to regulate ATF4 expression.* Int J Mol Med, 2019. **43**(1): p. 345-357.
23. Zhu, G., et al., *MicroRNA-224 Promotes Pancreatic Cancer Cell Proliferation and Migration by Targeting the TXNIP-Mediated HIF1alpha Pathway.* Cell Physiol Biochem, 2018. **48**(4): p. 1735-1746.
24. Liu, Y.B., et al., *Silencing long non-coding RNA MEG3 accelerates tibia fraction healing by regulating the Wnt/beta-catenin signalling pathway.* J Cell Mol Med, 2019. **23**(6): p. 3855-3866.
25. Sun, X., et al., *Down-regulation of lncRNA MEG3 promotes endothelial differentiation of bone marrow derived mesenchymal stem cells in repairing erectile dysfunction.* Life Sci, 2018. **208**: p. 246-252.
26. Wang, Y. and D. Kong, *Knockdown of lncRNA MEG3 inhibits viability, migration, and invasion and promotes apoptosis by sponging miR-127 in osteosarcoma cell.* J Cell Biochem, 2018. **119**(1): p. 669-679.
27. Liu, Y., et al., *Upregulation of long noncoding RNA MEG3 inhibits the osteogenic differentiation of periodontal ligament cells.* J Cell Physiol, 2019. **234**(4): p. 4617-4626.
28. Duan, Y., et al., *PC-3-Derived Exosomes Inhibit Osteoclast Differentiation by Downregulating miR-214 and Blocking NF-kappaB Signaling Pathway.* Biomed Res Int, 2019. **2019**: p. 8650846.
29. Peng, R., et al., *miR-214 down-regulates ARL2 and suppresses growth and invasion of cervical cancer cells.* Biochem Biophys Res Commun, 2017. **484**(3): p. 623-630.

30. Zhang, J., et al., *miR-214 promotes apoptosis and sensitizes breast cancer cells to doxorubicin by targeting the RFWD2-p53 cascade.* Biochem Biophys Res Commun, 2016. **478**(1): p. 337-342.

Table

Table 1 Primer sequence

Gene	Primer sequence
MEG3	F: 5’-ATCCGTCCACCTTGTCT-3’
	R: 5’-CCTCTTCATCCTTTGCCATC-3’
miR-214	F: 5’-GACAGCAGGCACAGACA--3’
	R: 5’-GTGCAGGGTCCGAGG-3’
TXNIP	F: 5’-GAAGCTCCTCCCTGCTATATGGA-3’
	R: 5’-CCATGTCATCTAGCAGAGGAGTTGT- 3’
U6	F: 5’-ATTGGAACGATACAGAGAAGATT-3’
	R: 5’-GGAACGCTTCACGAATTTG-3’
GAPDH	F: 5’-ACGGCAAGTTCAACGGCACAG-3’
	R: 5’-GACGCCAGTAGACTCCACGACA-3’

Note: F, forward; R, reverse; MEG3, maternally expressed gene 3; miR-214, microRNA-214; TXNIP, thioredoxin-interacting protein; GAPDH, glyceraldehyde-3-phosphate dehydrogenase.

Figures

Figure 1

MEG3 and TXNIP are overexpressed while miR-214 is underexpressed in femoral tissues of OP rats. A. Detection of MEG3 expression of rat femoral tissues in each group by RT-qPCR; B. Detection of miR-214 expression of rat femoral tissues in each group by RT-qPCR; C. Detection of TXNIP mRNA expression of rat femoral tissues in each group by RT-qPCR; D. Protein bands of TXNIP of rat femoral tissues in each group; E. Detection of TXNIP protein expression of rat femoral tissues in each group by Western blot analysis; a, $P < 0.05$ vs the sham group; b, $P < 0.05$ vs the si-NC group; c, $P < 0.05$ vs the mimics NC group; d, $P < 0.05$ vs the OE-MEG3 + mimics NC group; data among multiple groups were analyzed by ANOVA, after which pairwise comparison was performed by LSD-t.

Figure 3

MEG3 silencing and miR-214 overexpression enhance BMD, BV/TV, Tb.N and Tb.Th of femoral tissues in OP rats. A. Maps of rat proximal femur microstructure in each group by micro-CT; B. Comparison of BMD in rat femoral tissues in each group; C. Comparison of BV/BT in rat femoral tissues in each group; D. Comparison of Tb.N in rat femoral tissues in each group; E. Comparison of Tb. Th in rat femoral tissues

in each group; a, P < 0.05 vs the sham group; b, P < 0.05 vs the si-NC group; c, P < 0.05 vs the mimics NC group; d, P < 0.05 vs the OE-MEG3 + mimics NC group; data among multiple groups were analyzed by ANOVA, after which pairwise comparison was performed by LSD-t.

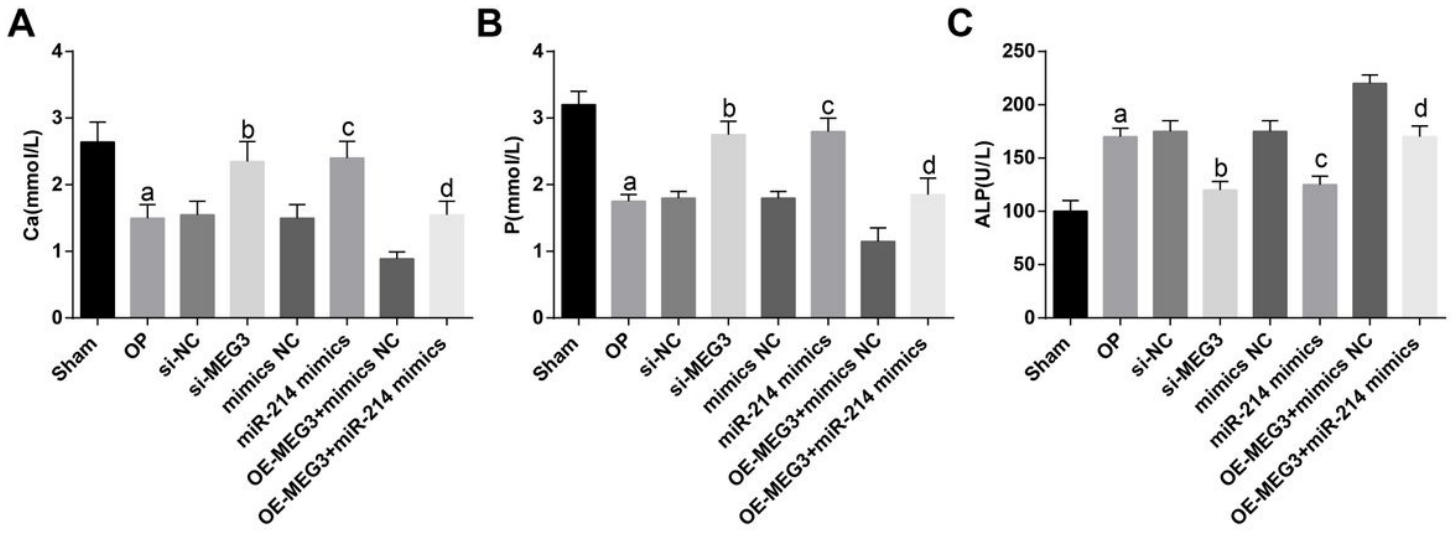

Figure 5

MEG3 silencing and miR-214 overexpression elevate Ca and P contents and reduce ALP content in OP rats' blood. A. Comparison of Ca content in blood samples of rats in each group; B. Comparison of P content in blood samples of rats in each group; C. Comparison of ALP content in blood samples of rats in each group; a, P < 0.05 vs the sham group; b, P < 0.05 vs the si-NC group; c, P < 0.05 vs the mimics NC group; d, P < 0.05 vs the OE-MEG3 + mimics NC group; data among multiple groups were analyzed by ANOVA, after which pairwise comparison was performed by LSD-t.

Figure 8

MEG3 silencing and miR-214 overexpression increase the number of osteoblasts and collagen area of femoral tissues in OP rats. A. Representative results of HE staining and Masson staining; B. Number of osteoblasts in rat femurs in each group; a, P < 0.05 vs the sham group; b, P < 0.05 vs the si-NC group; c, P < 0.05 vs the mimics NC group; d, P < 0.05 vs the OE-MEG3 + mimics NC group; data among multiple groups were analyzed by ANOVA, after which pairwise comparison was performed by LSD-t.

Figure 10

MEG3 silencing and miR-214 overexpression upregulate OPG protein expression and downregulate PANKL protein expression of femoral tissues in OP rats. A. Detection of OPG and PANKL protein expression in rat femoral tissues by immunohistochemical staining; B. Protein bands of OPG and PANKL in rat femoral tissues by Western blot analysis; C. Comparison of OPG/PANKL values of rat femoral

tissues in each group; a, P < 0.05 vs the sham group; b, P < 0.05 vs the si-NC group; c, P < 0.05 vs the mimics NC group; d, P < 0.05 vs the OE-MEG3 + mimics NC group; data among multiple groups were analyzed by ANOVA, after which pairwise comparison was performed by LSD-t.

Figure 12

Results of osteoblast isolation. A. Observation of osteoblasts climbing out of the femoral tissues 7 d after adherence by the inverted microscope; B. Observation of the 4th passage osteoblasts by the inverted microscope; C. Representative figure of COL-I staining; D. Representative figure of Gomori staining; E. Representative figure of ARS staining.

Figure 13

MEG3 silencing and miR-214 overexpression strengthen osteoblast viability. A. Protein bands of PCNA and cyclin D1 in each group; B. Comparison of PCNA and cyclin D1 protein contents in each group; C. Representative results of EdU staining; D. Comparison of OD values in each group; E. Comparison of cell proliferation rates in each group; a, P < 0.05 vs the control group; b, P < 0.05 vs the si-NC group; c, P < 0.05 vs the mimics NC group; d, P < 0.05 vs the OE-MEG3 + mimics NC group; data among multiple groups were analyzed by ANOVA, after which pairwise comparison was performed by LSD-t.

Figure 15

MEG3 silencing and miR-214 overexpression enhance COL-I and COL-X contents and decrease COL-II content of osteoblasts. A. Immunocytochemical detection of COL-I, COL-II and COL-X contents in each group; B. Comparison of COL-I, COL-II and COL-X contents in each group; a, P < 0.05 vs the control group; b, P < 0.05 vs the si-NC group; c, P < 0.05 vs the mimics NC group; d, P < 0.05 vs the OE-MEG3 + mimics NC group; data among multiple groups were analyzed by ANOVA, after which pairwise comparison was performed by LSD-t.

Figure 17

MEG3 silencing and miR-214 overexpression improve osteoblast differentiation ability. A. Protein bands of OCN, RUNX2 and Osteolix of rat osteoblasts in each group; B. Comparison of OCN, RUNX2, and Osteolix protein contents of rat osteoblasts in each group; C. Representative results of ALP staining with BCIP/NBT kit and alizarin red staining; D. Comparison of ALP activity of rat osteoblasts in each group; E. Comparison of mineralized nodule area of rat osteoblasts in each group; a, P < 0.05 vs the control group; b, P < 0.05 vs the si-NC group; c, P < 0.05 vs the mimics NC group; d, P < 0.05 vs the OE-MEG3 + mimics

NC group; data among multiple groups were analyzed by ANOVA, after which pairwise comparison was performed by LSD-t.

Figure 20

MEG3 specifically binds to miR-214. A. Prediction of the binding site between MEG3 and miR-214 by the bioinformatics software; B. Verification of the regulatory relationship between MEG3 and miR-214 by dual luciferase reporter gene assay; C. Verification of the binding relationship of MEG3 and miR-214 in osteoblasts by RNA-pull down assay to; D. MEG3 and miR-214 expression of osteoblasts in each group; a, $P < 0.05$ vs the sham group; b, $P < 0.05$ vs the si-NC group; c, $P < 0.05$ vs the mimics NC group; d, $P < 0.05$ vs the OE-MEG3 + mimics NC group; data between two groups were compared by t-test, and those among multiple groups by ANOVA, after which pairwise comparison was performed by LSD-t.

Figure 21

MiR-214 targets TXNIP. A. Online prediction of binding site between TXNIP and miR-214; B. Verification of the regulatory relationship between miR-214 and TXNIP by dual luciferase reporter gene assay; C. Comparison of TXNIP mRNA expression of osteoblasts in each group; D. Protein bands of TXNIP; E. Comparison of TXNIP protein content of osteoblasts in each group; a, $P < 0.05$ vs the sham group; b, $P < 0.05$ vs the si-NC group; c, $P < 0.05$ vs the mimics NC group; d, $P < 0.05$ vs the OE-MEG3 + mimics NC group; data between two groups were compared by t-test, and those among multiple groups by ANOVA, after which pairwise comparison was performed by LSD-t.